A&A 395, 915–927 (2002)
DOI: 10.1051/0004-6361:20021313

Astronomy & Astrophysics

H_2O in stellar atmospheres

II. ISO spectra of cool red giants and hydrostatic models⋆

B. Aringer[1], F. Kerschbaum[2], and U. G. Jørgensen[1]

[1] Niels Bohr Institute, Astronomical Observatory, Juliane Maries vej 30, 2100 Copenhagen, Denmark
e-mail: uffegj@nbi.dk
[2] Institut für Astronomie der Universität Wien, Türkenschanzstrasse 17, 1180 Wien, Austria
e-mail: kerschbaum@astro.univie.ac.at

Received 1 May 2002 / Accepted 5 September 2002

Abstract. We present 26 ISO-SWS spectra taken from a sample of 13 M-type Semiregular, Lb and Mira variables and covering the wavelength range between 2.36 and 5 μm at a medium resolution. All of the studied objects show intense water bands producing a deep absorption dip around 2.5 μm. Features of CO, OH, SiO and CO_2 are also visible. Using the new H_2O linelist published in the first paper of this series and available opacity data for the other important molecules, we calculated a grid of hydrostatic MARCS atmospheres and the corresponding synthetic ISO-SWS spectra. Based on the comparison with these theoretical results the ISO observations can be divided into four classes. The first two groups include the spectra of the Semiregular (SRb) and Lb variables in our sample. For all of them the region between 2.36 and 4.2 μm can be quite well reproduced by our hydrostatic models. Only the predicted SiO bands above 4 μm are in some cases too strong which is due to known dynamical effects. Depending on the temperature (above or below 3000 K) of the atmosphere, which mainly determines the intensity of the water depression at 2.5 μm, the spectra of the Semiregular and Lb variables fall into the first or second class. The third group consists of observations of Mira stars obtained around maximum light where the range between 2.36 and 4.2 μm can be fitted with our MARCS models except for a strong emission bump appearing in the ISO-SWS data in the region of the SiO features and the slope very close to the short wavelength border. Finally, the last type of spectra corresponds to Mira variables during the phases around the minimum of their visual light curve. For this class the observed water absorption at 2.5 μm is much more intense than in any hydrostatic atmosphere with a realistic choice of effective temperature and surface gravity. Thus, we conclude that dynamical models are needed to explain the ISO-SWS data of Mira stars. For all of the cooler objects from our sample the predicted CO_2 bands between 4.2 and 4.6 μm are too weak which may be due to the opacity data.

Key words. infrared: stars – stars: atmospheres – stars: late type

1. Introduction

Together with TiO, water dominates the opacity in the atmospheres of all cool oxygen-rich stars. This is mainly due to the combination of the huge number of spectral lines these molecules have with their relatively high abundances. In both cases millions of transitions give rise to a significant absorption distributed over broad regions in the spectra. For H_2O the large quantity of lines is connected to its non-linear geometry introducing additional degrees of freedom for the vibrational-rotational motion, while for TiO the incorporation of several electronic states is the important factor. The role of water in stellar atmospheres has been discussed in the first paper of this series (Paper I, Jørgensen et al. 2001). Reviews concerning TiO can be found in Plez (1998) or Jørgensen (1994). While the strong bands of TiO are situated in the range below 1 μm and cause a substantial heating of the atmospheres (see e.g. Aringer et al. 1997), the H_2O absorption dominates the whole infrared region from 1.5 up to 20 μm and more, cooling the matter significantly down. Intense features of water appear at temperatures around 3200 to 3400 K which is lower than for TiO.

In Paper I we have published an extensive list of water lines suitable for the determination of opacities needed for the construction of model atmospheres as well as for the calculation of synthetic spectra. The intensities and shapes of the bands at different temperatures are compared to the experimental data collected in HITRAN and HITEMP (Rothman et al. 1992) as well as to results obtained from the NASA AMES list presented by Partridge & Schwenke (1997). While HITRAN contains only a small fraction of the transitions that produce the

Send offprint requests to: B. Aringer, e-mail: aringer@alf.nbi.dk
⋆ Based on observations with ISO, an ESA project with instruments funded by ESA Member States with participation of ISAS and NASA. The SWS is a joint project of SRON and MPE.

H_2O absorption in the relatively hot environment of a stellar atmosphere, the situation for HITEMP is much better. However, concerning the opacities needed to compute model structures also HITEMP is not complete enough. In general the overall intensities and shapes of the water features based on the NASA AMES and our list agree very well. There are certain differences in the infrared discussed in Paper I.

Since water is also one of the main absorbers in the atmosphere of the earth, it is usually not easy to observe its broad features in the infrared with ground-based telescopes. An excellent tool to study the H_2O bands at lower frequencies are the spectra taken by the Short Wavelength Spectrometer (ISO-SWS, de Graauw et al. 1996) aboard the Infrared Space Observatory (ISO), which cover the range between 2.4 and 45.2 μm. ISO-SWS data of the Semiregular variable SV Peg have already been shown in Paper I in order to compare results from different linelists. In this work we present a more systematic investigation concerning water in the ISO spectra of cool oxygen-rich red giants, most or all of which are probably AGB stars. The big advantage of these objects is that many of them are quite bright in the infrared. As a consequence there exists a considerable number of reliable ISO-SWS observations. The problem associated with the AGB stars is that all of them show strong pulsations and mass loss which can not be described by hydrostatic model atmospheres (e.g. Höfner & Dorfi 1997; Höfner 1999). This will also affect the molecular spectra (e.g. Aringer et al. 1999) depending on the intensity of the variations, the species and the wavelength range. Therefore, in the present paper we will investigate the successes and limitations of hydrostatic models concerning the reproduction of the observed water bands.

Tsuji et al. (1999) have studied the water features in the ISO-SWS spectra of several cool AGB variables. They also found that the bands can not always be fitted with their classical hydrostatic atmospheres. Thus, in order to remove the discrepancies they introduced the scenario of a warm molecular envelope (Tsuji et al. 1997) which consists of one or more layers situated above the photosphere. Based on this approach Matsuura et al. (2002) produced fits to the ISO-SWS data and studied the variability of four Mira stars covering the range between 2.5 and 4.0 μm. At this point we want to emphasize that the atmospheres of such objects have a complex dynamical structure which offers a natural explanation for the problems with the hydrostatic models and can not be consistently described by the simple addition of molecular shells with constant temperature and density. Thus, an upcoming paper of this series will include a discussion of Mira spectra based on recent non-grey dynamical computations (e.g. Höfner 1999).

2. Observations of cool O-rich variables

In order to compare the synthetic spectra discussed in the following section to observational results we used the data from five open time ISO projects (*fkerschb.orichsrv/orichsrl/zzagb2pn* and *jhron.varlpv/varlpv2*) for our work. It was an aim of these programs to cover on one hand a large number of representative cool O-rich variables with different pulsational properties (Mira, SRa, SRb, Lb and OH/IR) and on the other hand to monitor a few objects to study their temporal behavior. In total 22 red giants, most or all of which are probably AGB stars, could be observed at least once. For ten of them between two and seven individual spectra taken at different phases are available. In this paper we present the data of 13 Mira, Semiregular (only SRb) and cool Irregular (Lb) variables which cover a wide range of pulsational properties, temperatures and mass loss rates. For seven of the objects there exists more than one observation. In total we used 26 spectra for this work. Since the pulsational properties of the SRb and Lb stars are quite similar (Kerschbaum et al. 2001), they will be treated here as a single group.

The observations were carried out with the ISO-SWS instrument (de Graauw et al. 1996) with full grating scans covering typically the wavelength range between 2.38 and 45.2 μm using AOT01 with speed 2. The intrinsic spectral resolution varies from 200 to 600 depending on frequency (Leech 1998; Valentijn et al. 1996). The pipeline processed data products (OLP 7) were further reduced with the ISO Spectral Analysis Package ISAP (Sturm et al. 1998). In general, for the preparation of the spectra presented here the connection of the individual sections which introduces an additional uncertainty was done by multiplying the longer wavelength band in order to fit the overlapping regions. Only for flux levels below 100 Jy we have applied the correction additively.

In Figs. 1 and 2 we present the ISO-SWS observations used for this paper. The wavelength range between 2.36 and 5 μm is shown, which includes the broad 2.5 μm absorption dip caused by water as well as bands of CO, SiO, OH and CO_2. The appearance of the different features will be discussed later in more detail. The fluxes are normalized to the value at 3.8 μm where the molecular opacity has a minimum. However, in very cool stars even this point will be affected by water absorption. The numerical resolution of the data is set to 450 which is typical for band one of the ISO-SWS (400 to 600) and will also be used for all synthetic and observed spectra presented later in this work. In Fig. 1 we show the observations of the Semiregular and Lb variables from our sample. In addition, two measurements of the Mira star R Aql are included which can also be found in Fig. 2. Multiple spectra of single objects are always collected in one panel. For those Semiregular and Lb variables where two observations exist it is obvious that especially the features around 2.5 μm (H_2O) and 4.5 μm (CO_2) change as a function of time. Even much larger variations appear for the Mira stars as the example of R Aql in Fig. 1 and the collection of spectra of R Aql and R Cas in Fig. 2 demonstrate.

3. Synthetic spectra

In order to compare our ISO data to synthetic spectra we have computed a small grid of cool and extended hydrostatic atmospheres using an improved version (Jørgensen et al. 1992) of the MARCS code (Gustafsson et al. 1975) with spherical radiative transfer routines from Nordlund (1984). Molecular opacities of CO, SiO, OH, TiO, H_2O and CN have been taken into account by treating them in the opacity sampling approximation (Jørgensen 1992). The calculated models are almost

identical to those presented and described by Aringer et al. (1997) in their work on SiO first overtone lines. The only major difference is the use of new opacity sampling data for TiO which were derived from an updated version (SCAN data base, Jørgensen 1997) of the original linelist (Jørgensen 1994) with recent f-values taken from Langhoff (1997). However, this change will not affect the infrared spectra significantly. It should be noted here that the molecular opacities in the model atmospheres (opacity sampling) and in the calculation of the synthetic spectra (from linelists) have been treated consistently which is a very important requirement to be able to obtain realistic results.

Our small grid of atmospheres covers the effective temperature range between 2600 and 4600 K and values of $\log(g[\mathrm{cm/s^2}])$ from 0.0 to −0.6. All models have one solar mass and solar chemical abundances. It was shown by Aringer et al. (1997) for the SiO bands that compared to the other parameters a possible variation of the stellar mass has only a small influence on the infrared molecular spectra, if one assumes the typical range expected for galactic AGB stars. This holds also for the water features around 2.5 μm, even when a spherical radiative transfer is applied to compute the synthetic spectra. The temperature range mentioned above was chosen to cover all giants from relatively warm ones where only CO dominates the molecular opacity in the infrared down to the coolest ones typically expected from evolutionary calculations.

Our synthetic spectra cover the wavelength range between 2.36 and 7.75 μm at a resolution of 300 000. Based on the atmospheric models mentioned above they were calculated using the program COMA (Aringer 2000), which allows us to derive molecular opacities directly from the different linelists, and a detailed spherical radiative transfer code (Windsteig et al. 1997). For the molecular transitions we assumed Doppler profiles and a microturbulent velocity of $\xi = 2.5$ km s^{-1} (see Aringer et al. 1997). Opacities of CO, SiO, OH, H_2O and CO_2 have been included in the computation. The lower limit of the selected spectral range corresponds to the short wavelength end of our ISO-SWS observations, while the upper limit was chosen to avoid regions which may be contaminated by the opacity originating from a circumstellar dust shell being present around many of the studied cool red giants with moderate mass loss (10 μm feature). In order to compare the theoretical results to the observed ISO data their original resolution of 300 000 was reduced to reproduce the wavelength grid of our ISO-SWS spectra (resolution of 450).

The following molecular lines have been included into our computations of the synthetic spectra. The isotopic abundances are taken from Anders & Grevesse (1989): in the case of CO we used ∼132 000 vibrational-rotational transitions for the seven isotopes $^{12}C^{16}O$, $^{12}C^{17}O$, $^{12}C^{18}O$, $^{13}C^{16}O$, $^{13}C^{17}O$, $^{13}C^{18}O$ and $^{14}C^{16}O$. They originate from a linelist prepared by Goorvitch & Chackerian (1994). For the two most important species $^{12}C^{16}O$ and $^{13}C^{16}O$ the latter contains all $\Delta V = 1$, 2 and 3 lines up to $V = 20$ and $J = 150$. The SiO list has already been discussed in Aringer et al. (1997). It consists of ∼93 000 vibrational-rotational transitions for the three isotopes $^{28}Si^{16}O$, $^{29}Si^{16}O$ and $^{30}Si^{16}O$, and it is complete up to $V = 15$ and $J = 251$. In order to calculate the opacity of OH we used a data base which includes ∼38 000 lines for the main isotope (Schwenke 1997). A detailed discussion concerning the linelist for H_2O is given in Paper I where also one of our ISO spectra is presented. The full data base consists of approximately three billion transitions for the main isotope. In order to save computation time we have selected the ∼19 466 000 lines with an intensity larger than 5×10^{-8} km/mol at 3500 K for the calculation of the synthetic spectra. This limit was chosen to be just low enough that there appears no noticeable change ($\ll 1\%$) of the results. Also the fact that we do not take the heavier isotopes into account will not have a visible effect on the spectra at the ISO-SWS resolution. In addition we produced some spectra using the water opacity from the NASA AMES list (Partridge & Schwenke 1997). For CO_2 there exists no computed linelist at the moment. Thus, we took the information from the 1996 version (CD-ROM) of the HITRAN data base which includes ∼61 000 lines (Rothman et al. 1992) and its high temperature extension HITEMP with ∼1 032 000 lines.

4. Results from model atmospheres

In Fig. 3 we present synthetic spectra for a temperature sequence with $\log(g[\mathrm{cm/s^2}]) = 0.0$ which have been calculated including only single selected species into the determination of the molecular absorption. All of them are based on the same model atmosphere which was constructed with the complete set of opacities. CO, OH, SiO and H_2O are shown. One should always be careful with the interpretation of such spectra, since neglecting the rest of the molecular opacities might change the geometrical depth where the investigated lines are formed. Nevertheless, it is still possible to get informations about the positions of the features and their approximate behavior as a function of stellar temperature. In the case of CO one can see that the absorption dip around 2.4 μm is already quite intense at 3600 K and it does not change very much, if the object becomes cooler. In order to get significantly weaker CO bands effective temperatures exceeding 4000 K are needed as long as the surface gravity and the chemical composition are not altered. The features of SiO and OH show similar characteristics concerning their behavior as a function of temperature. In the model with $T_{\mathrm{eff}} = 3100$ K they are relatively intense, and from our calculations we do not expect any major changes for cooler stars. On the other hand one can clearly see that the SiO and OH bands are much weaker at 3600 K. Above 4000 K they start to disappear. H_2O will only be observed in cool objects with effective temperatures below 3300 to 3400 K. It produces a broad absorption dip around 2.5 μm and dominates the molecular opacity in the whole ISO-SWS range at $T_{\mathrm{eff}} \leq 3000$ K. Even below 2600 K the water bands still become more intense with decreasing temperature.

As one can see in Fig. 2 the ISO-SWS observations of cool Mira stars show an intense and broad absorption dip between 4.15 and 4.6 μm which is due to CO_2. It appears also in the spectra of relatively warm Lb or Semiregular variables like SV Peg where it is quite weak. In the models the calculated CO_2 bands occur only in the coolest stars with $T_{\mathrm{eff}} < 3000$ K. However, they are in all cases predicted much too weak. As a consequence the spectral range between 4.2 and 4.6 μm can

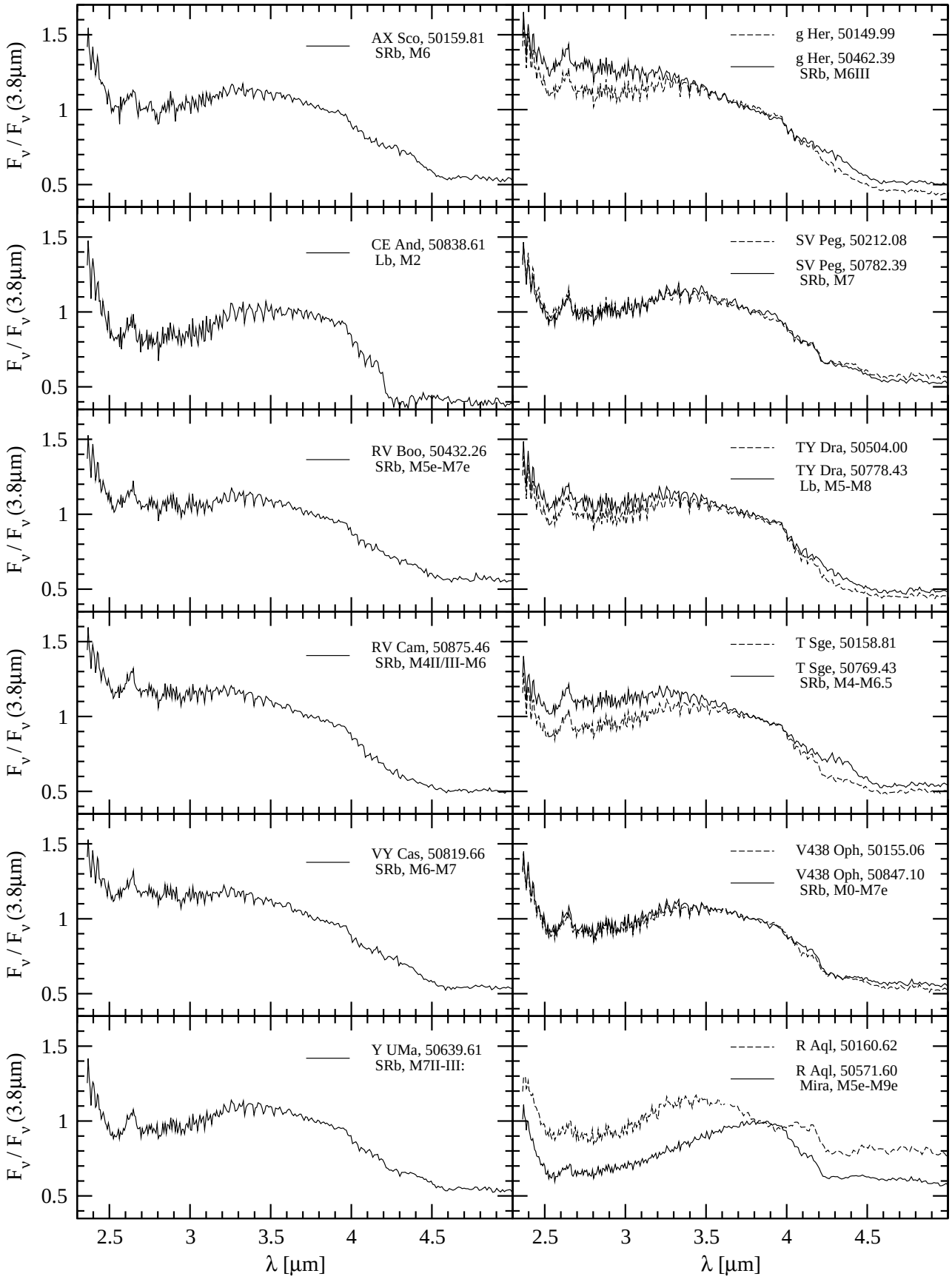

Fig. 1. ISO-SWS spectra for the SRb and Lb variables of our sample and for two phases of the Mira star R Aql. The fluxes are normalized to the value at 3.8 μm. Multiple observations of single objects are collected in one panel. The Julian date (JD−2 400 000) is given for each spectrum. Information on the spectral and variability type is also included.

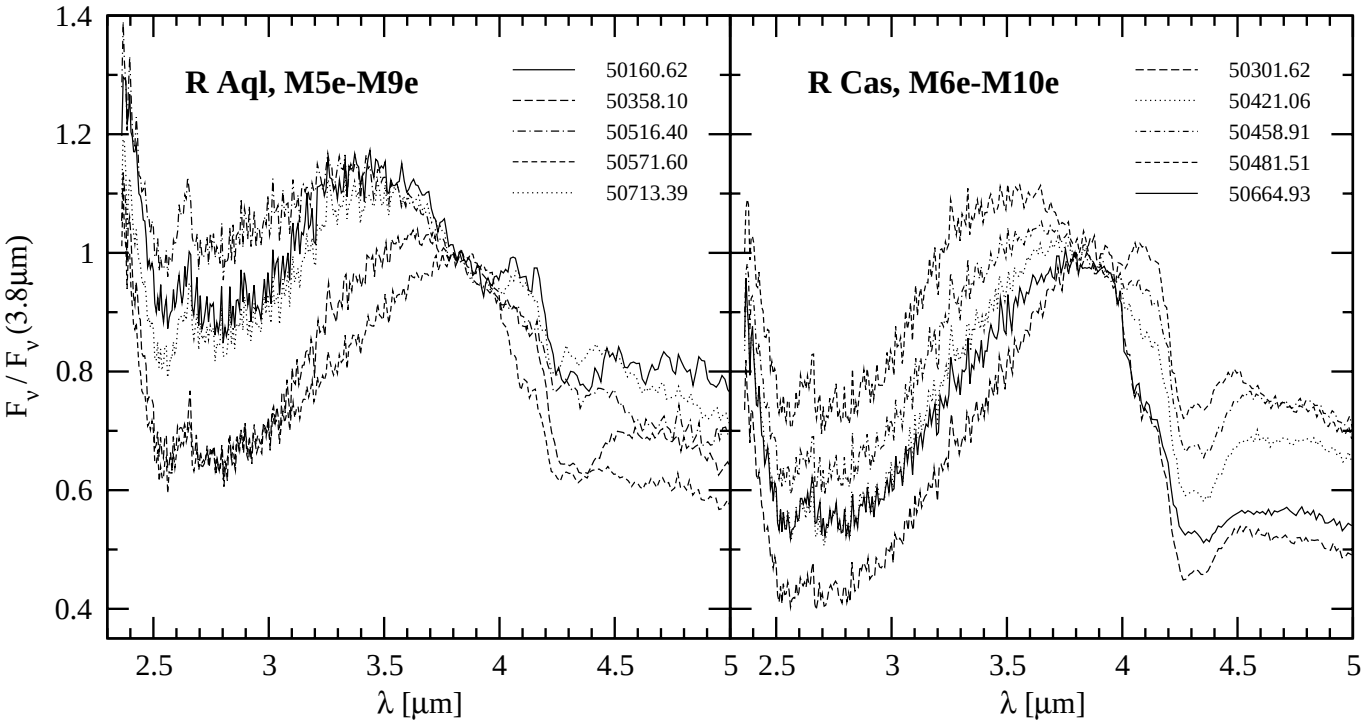

Fig. 2. ISO-SWS spectra of the two Mira stars R Cas and R Aql taken at different epoch. The fluxes are normalized to the value at 3.8 μm. The Julian date (JD−2 400 000) is given for each spectrum.

not be reproduced at all, and was therefore excluded from this study. The problem may be caused by the use of an incomplete CO_2 linelist, since the HITRAN data are a collection of a limited number of transitions measured at low temperatures. Especially for molecules with many lines such a compilation may only include a fraction of the real opacity present in a hot stellar environment. For water this is demonstrated in Paper I where also a more detailed discussion on the topic can be found. However, for the two species mentioned here, CO_2 and H_2O, a high temperature extension of HITRAN is available, which is called HITEMP and includes a significantly larger number of transitions. In the case of water the use of lines from HITEMP instead of HITRAN gives synthetic spectra which are much closer to the results based on a complete theoretical list. Nevertheless, the opacity produced by millions of weak lines creating an almost continuous absorption over broad wavelength ranges is still clearly underestimated. As it has already been mentioned there exists no complete computed linelist for CO_2 at the moment. Compared to HITRAN calculations based on the HITEMP data produce somewhat more intense bands, which are still much weaker than the observed ones. Since CO_2 has a much smaller effect on the stellar atmosphere than water, which adjusts the structure corresponding to its absorption, the contribution of many weak lines will be more important for the resulting intensities of the features, if a consistent computation is applied where the same opacity sources are used for the model and the synthetic spectrum.

Another possible explanation for the inability of our MARCS models to reproduce the CO_2 bands of the observed red giants is the fact that hydrostatic structures may underestimate the density in the cool outer layers by orders of magnitude. This is connected to the dynamical nature of these objects, and it will be discussed later as the reason for the extremely intense water absorption appearing in the ISO-SWS spectra of Mira variables at certain phases. As it turns out the ISO observations of the CO_2 features in the mid infrared, which are situated between 13 and 16 μm, indicate the existence of such relatively dense regions with excitation temperatures of about 600 K around AGB stars with strong pulsations (Ryde et al. 1999; Cami et al. 2000). Concerning the CO_2 depression at 4.5 μm the effect of these layers has to be really very large in the coolest giants and it needs to be already important in many Semiregular and Lb variables where the H_2O bands can easily be fitted by using only the hydrostatic models. In this context it should be noted that Aringer et al. (1999) found that it is necessary to apply dynamical atmospheres in order to reproduce the first overtone SiO bands of Semiregular stars.

In Fig. 4 we present a sequence of synthetic ISO spectra calculated from three MARCS atmospheres with different effective temperatures. All models have one solar mass, solar chemical abundances and $\log(g[\mathrm{cm/s^2}]) = 0.0$. It is obvious that the molecular absorption in the whole wavelength range increases significantly for cooler objects. The spectra are normalized to the flux at 3.8 μm where the molecular opacity has a minimum. It should be noted that for $T_{\rm eff} \leq 3000$ K there exists no point between 2 and 8 μm where the spectrum reaches the continuum level. As one can see in Fig. 3 this is mainly due to the opacity of water which affects the complete wavelength interval at low temperatures. In warmer stars it is possible to find such continuum points in the region around 3.8 μm, which may still be contaminated by some of the OH features that are visible in the 3600 K spectrum in Fig. 3. However, these are very

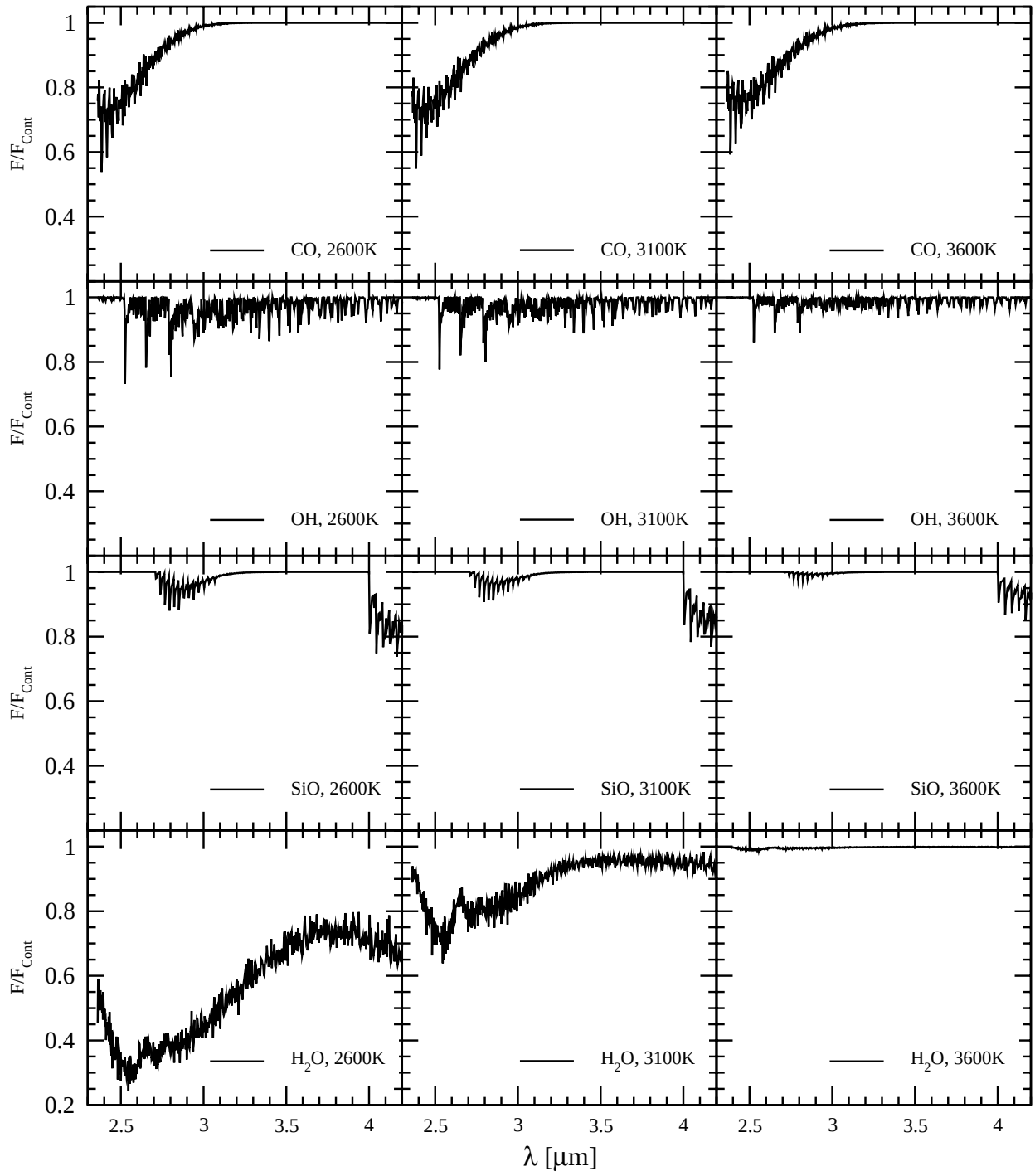

Fig. 3. Synthetic spectra for the ISO-SWS range, which have been calculated from MARCS atmospheres with three different effective temperatures by including only the molecular opacity of a single species. The bands of CO, OH, SiO and water are shown. The spectra are normalized to a continuum defined by a computation without molecular and atomic lines. All models have $\log(g[\mathrm{cm/s^2}]) = 0.0$, one solar mass and solar chemical abundances.

distinct and narrow bands that can be easily separated from the surrounding continuum. The most intense molecular absorption appears at 2.5 μm. This is caused by CO which produces its features already in relatively hot stars and by water which occurs only at lower temperatures. In the range between 2600 and 3300 K the depth of the depression around 2.5 μm depends very much on $T_{\rm eff}$.

In Fig. 5 we show synthetic ISO-SWS spectra as a function of $\log(g)$ for three MARCS models with $T_{\rm eff}$ = 2800 K, one solar mass and solar chemical abundances. They are again normalized to the flux at 3.8 μm. As one can see, the molecular absorption becomes slightly weaker at lower surface gravities. The differences are small compared to the changes related to temperature, and they are caused by emission components in the lines which are due to sphericity effects

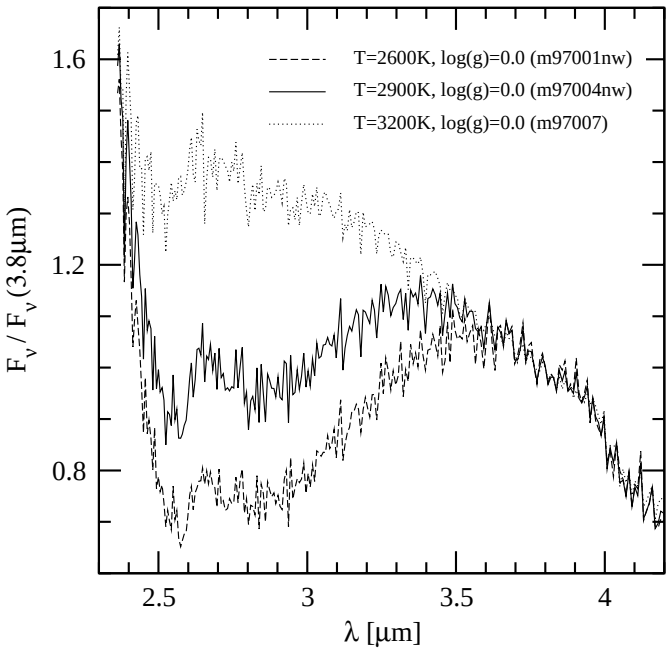

Fig. 4. Synthetic ISO-SWS spectra calculated from MARCS atmospheres with three different effective temperatures. The fluxes are normalized to the value at 3.8 μm. All models have $\log(g[\mathrm{cm/s^2}]) = 0.0$, one solar mass and solar chemical abundances. The designations of the atmospheres are also indicated.

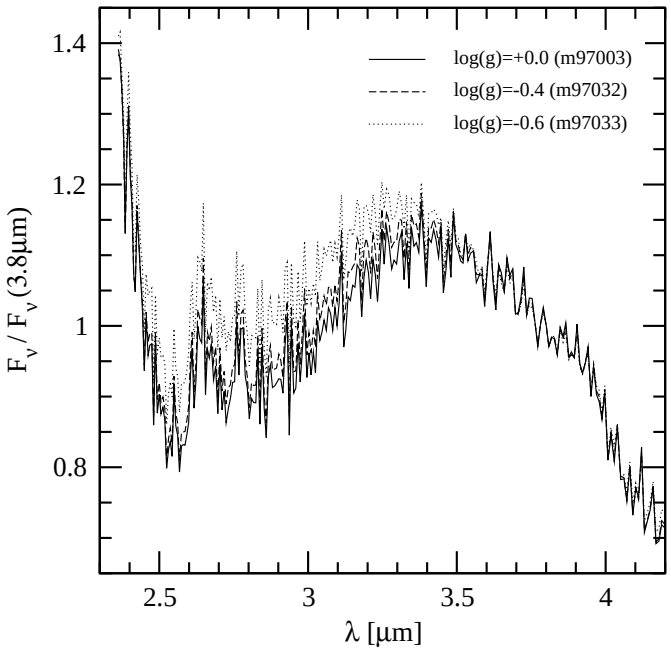

Fig. 5. Synthetic ISO-SWS spectra calculated from MARCS atmospheres with an effective temperature of 2800 K and three different values of $\log(g[\mathrm{cm/s^2}])$ which are typical for cool giants. The fluxes are normalized to the level at 3.8 μm. All models have one solar mass and solar chemical abundances.

appearing in very extended hydrostatic atmospheres. In the case of SiO this phenomenon is discussed in Aringer et al. (1999). For more compact objects where sphericity effects are only of minor importance the intensity of the depression around 2.5 μm increases with lower values of $\log(g)$. This is demonstrated in Fig. 6 where we compare a 2800 K dwarf to a giant. In general one can say that the influence of the surface gravity on our synthetic AGB star spectra is relatively small, and concerning the appearance of the absorption feature at 2.5 μm it corresponds to a small change of the effective temperature.

We have also investigated the influence of the microturbulent velocity on the final results by adopting different values between 2.5 and 5.0 km $\mathrm{s^{-1}}$, which is already a rather high selection regarding the line broadening observed in red giants. Since we only included these changes into the determination of the spectra and not into the model calculation, we obtained upper limits for the effect. Compared to a self-consistent treatment of the opacities the latter will always be overestimated by such an approach. As it turns out, an increase of ξ from 2.5 to 5.0 km $\mathrm{s^{-1}}$ produces only minor variations concerning the appearance of the water bands in the normalized spectra. This result is not unexpected, because the H_2O absorption is mainly generated by a huge number of overlapping weak transitions. Significant differences could only be found in a narrow region below 2.5 μm where there are many strong CO lines, which will be more affected by an additional broadening. Compared to our reference point at 3.8 μm the intensity in this range decreases for $\xi = 5.0$ km $\mathrm{s^{-1}}$ by about 12 to 14%, while in the other parts of the spectrum the changes always remain below 5 to 7%.

5. Models and observations

In order to get some informations about the stellar temperatures we have compared the synthetic spectra calculated from our grid of hydrostatic MARCS atmospheres to the ISO-SWS data in the range between 2.36 and 4.2 μm. This was done by selecting for each observation the model which gives the best representation of the overall energy distribution. As it has just been mentioned this region is dominated by the intense molecular absorption from CO and water. Since the shape of the spectra changes significantly as a function of stellar temperature, even a difference of 50 K, which corresponds to the resolution of our grid, can be clearly seen. Due to uncertainties of the used linelists that will be discussed in a following section the intensity and appearance of the small scale structure of the H_2O bands was not taken into account for the comparison of theoretical and observed results. We did not extend our study to longer wavelengths, because we wanted to avoid problems with the CO_2 feature around 4.4 μm where the opacity might be significantly underestimated in all models of cool stars (see previous section). In addition, the region between 5.0 and 8.5 μm where the intense silicate dust emission starts does not include any well pronounced broad molecular absorption structures like the 2.5 μm H_2O depression, except for the SiO ground state bands above 7.5 μm. It is rather dominated by a quasi-continuous water opacity with a lot of small scale features (Aringer 2000). The results for four representative observations can be seen in Fig. 7 where we show the ISO-SWS data together with the synthetic spectra which give the best fit in the investigated frequency range. It should be noted that the good agreement concerning the overall energy distribution appearing

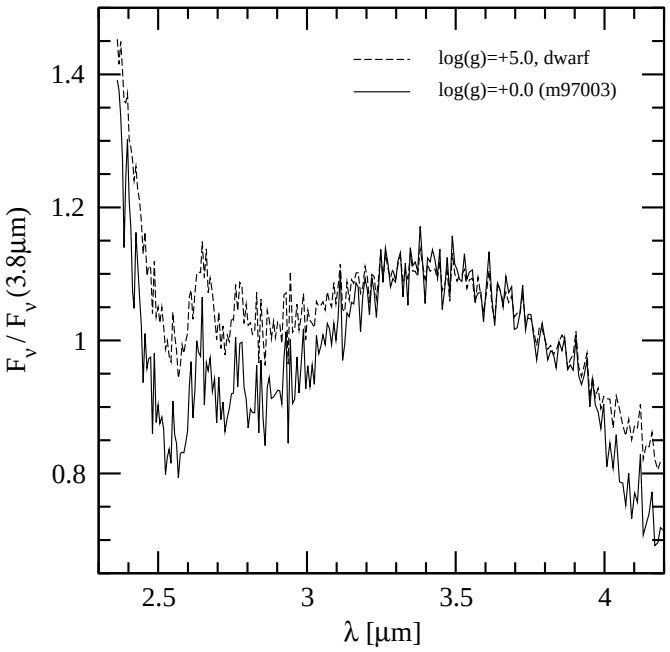

Fig. 6. Synthetic ISO-SWS spectra calculated from MARCS atmospheres. A giant with $\log(g[\mathrm{cm/s^2}]) = 0.0$ and a dwarf with $\log(g[\mathrm{cm/s^2}]) = +5.0$ are compared. The fluxes are normalized to the value at 3.8 μm. Both models have 2800 K, one solar mass and solar chemical abundances.

for the two Semiregular variables displayed in the upper panels of Fig. 7 could also be obtained for all other investigated stars of this type (SRb and Lb). All spectra are normalized to the flux level at 3.8 μm. Due to the strong variation of the overall shape as a function of the stellar temperature the latter can be defined with an accuracy of ±50 K, which corresponds to the grid resolution, if $\log(g[\mathrm{cm/s^2}]) = 0.0$ and solar chemical abundances are assumed. In reality many of the stars may be more extended which could decrease the values by up to 100 K for the typical parameter range expected for AGB objects (see previous section). Thus, the main source of errors which may then become up to 150 K are the uncertainties of $\log(g)$. However, also the C/O ratio could play a role, if it approaches values close to one. Due to the spectral variability of the objects the determined temperatures will also differ as a function of time. For the Semiregular and Lb stars in our sample, where we have more than one observation, the values change between 50 and 100 K, while in the Mira stars the variations are much larger.

Concerning the fit of spectra calculated from hydrostatic atmospheres we found four categories of ISO-SWS data. The spectral classification and the temperatures we derived for our observations are listed in Table 1. Representative examples for the four different types of spectra are shown in Fig. 7 where we compare measurements and theoretical results.

5.1. Type 1

The first group of spectra are those of Semiregular and Lb variables, which can be reproduced by hydrostatic MARCS models with effective temperatures between 3000 and 3200 K. They show water absorption in the 2.5 μm region. However, the H_2O bands are still relatively weak and do not dominate this wavelength range. Features of CO (around 2.4 μm), SiO (above 4.0 μm) and OH (in the whole interval) are also quite prominent. In all cases we could obtain very good fits to the observed spectra. Only the SiO bands are predicted a bit too strong, which is most probably a first consequence of dynamical phenomena, even in the Semiregular and Lb variables with their relatively weak pulsations. Aringer et al. (1999) explained the much too weak SiO features observed in all AGB stars by emission components in the molecular lines originating from the extended outer regions of dynamical atmospheres.

A good example for a star with spectra belonging to the first group is g Her which is also shown in Fig. 7. For the two observations of this object we obtained 3050 and 3150 K. The latter value is the highest one that we found for a star from our sample. It is in agreement with Tsuji et al. (1994), who adopted a temperature of 3200 K for g Her, and with the results from Plez et al. (1992), who got 3235 K using infrared fluxes and hydrostatic atmospheres. It should be mentioned that Plez et al. need a slightly warmer model (3300 K) to fit the TiO bands at shorter wavelengths. We find a similar trend for our calculations when we compare the results presented here for the spectra of type 1 and 2 with temperatures derived from TiO features of Semiregular variables in the optical range (Schultheis et al. 1999).

5.2. Type 2

The second group consists of spectra of Semiregular and Lb variables that can be reproduced by hydrostatic models with temperatures between 2700 and 3000 K. The water absorption is very intense and dominates the whole range below 3.5 μm. Features of CO, SiO and OH are still visible. Also for this type of spectra the agreement between calculations and observations is quite good with the exception that the predicted SiO bands above 4.0 μm are too strong. In general, the discrepancy concerning the SiO features is a bit larger than for the first group.

For some of the spectra we found that the observed and computed slopes close to the short wavelength boundary are different. In all of these cases the calculations predict too steep energy distributions for the narrow region below 2.4 μm, even if the results from ISO-SWS observations and model atmospheres look very similar in the rest of the studied frequency interval. However, since we are talking about a range situated directly at the edge of the ISO spectra, there might well be some uncertainties concerning the calibration for objects with steep gradients at the short wavelength boundary. We do not think that the discrepancies are due to the water opacity, because they appear only for a part of the data and computations with other linelists (Partridge & Schwenke 1997 and HITEMP) give almost the same slope below 2.4 μm. It should be noted that for the spectra of the first group and for earlier red giants (Decin et al. 1997), all of which have flatter gradients, such problems do not exist. In principle it could also be possible that in some type 2 observations the slopes in this region

Table 1. List of ISO-SWS spectra studied for this work. The first two columns include the names of the stars as well as the Julian dates of the observations. In the third column we give the effective temperatures derived from a fit of the ISO data using hydrostatic MARCS atmospheres. It is also indicated, if the water absorption is more (much more: $\ll$; just a bit more: $\leq$) intense than in the coolest models. The type corresponds to the four classes of spectra defined in the text. In the next column the presence of an emission bump in the region of the SiO bands is indicated. (+) means a weak emission feature. For the two Mira stars we have also included the visual phases taken from their AAVSO light curve.

Star	JD 2 400 000+	T [K]	Type	SiO	Phase
CE And	50838.61	2750	2		
R Aql	50160.62	2850	3	+	0.93
R Aql	50358.10	$\leq$2600	3	+	0.64
R Aql	50516.40	2950	3	+	0.21
R Aql	50571.60	<2600	4		0.40
R Aql	50713.39	2800	3	+	0.90
RV Boo	50432.26	3000	1		
RV Cam	50875.46	3100	1		
R Cas	50301.62	$\ll$2600	4		0.50
R Cas	50421.06	<2600	4	(+)	0.79
R Cas	50458.91	$\leq$2600	3	+	0.88
R Cas	50481.51	2650	3	+	0.93
R Cas	50664.93	<2600	4		0.36
VY Cas	50819.66	3100	1		
TY Dra	50504.00	2900	2		
TY Dra	50778.43	3000	1		
g Her	50149.99	3050	1		
g Her	50462.39	3150	1		
V438 Oph	50155.06	2850	2		
V438 Oph	50847.10	2900	2		
SV Peg	50212.08	2950	2		
SV Peg	50782.39	2900	2		
AX Sco	50159.81	2950	2		
T Sge	50158.81	2850	2		
T Sge	50769.43	3000	1		
Y UMa	50639.61	2900	2		

are influenced by dynamical effects weakening the absorption of CO or H_2O significantly.

5.3. Type 3

The third group is formed by spectra of Mira stars which can be reproduced with cool MARCS models having effective temperatures between 2600 and 3000 K. As in the case of type 2, intense water absorption dominates the whole wavelength range below 3.5 μm. The features of CO and OH are in general relatively weak, or sometimes even not visible. Only in the data set corresponding to the warmest model (R Aql, 50516.40) they are more pronounced. The reason for this weakening of the CO and OH bands are the large optical depth of the water absorption in the outer atmosphere, which does also affect the computed spectra, as well as dynamical phenomena (see e.g. the discussion of OH in Lebzelter et al. 2001).

In the region of the SiO first overtone transitions between 4.0 and 4.2 μm all data of type 3 show a broad strong emission bump. This feature has also been found by Yamamura et al. (1999) in an ISO observation of *o* Cet which is the prototype of all Mira stars. It should be noted that the discussed range includes the border between ISO-SWS bands 1e and 2a situated around 4.06 μm which may introduce some errors concerning small scale structures and the overall slope in the spectra. Nevertheless, since the bump is larger than the expected uncertainties and, as it will be discussed later, its appearance is correlated with the pulsation phase, we conclude that it is definitely not an artefact. In addition, it can only be seen in Mira variables. Thus, we have a clear indication for SiO emission in Mira stars visible in periods with relatively weak (compared to type 4) water absorption. It is obvious that the feature between 4.0 and 4.2 μm does not reflect the typical band structure appearing in the synthetic spectra and in the ISO-SWS data of the first two groups. This is a possible explanation, why Aringer et al. (1999) did not find any objects with SiO emission in their sample. Their way of defining the continuum by using certain regions between the bandheads will suppress broader structures. In this context it is interesting that in contrast to the behavior in hydrostatic atmospheres the molecular features in dynamical models can sometimes change their shapes significantly, especially if emission is involved. Thus, the absence of the typical SiO bandheads is not really unexpected. In their work on individual SiO lines observed in high resolution FTS spectra of Mira and Semiregular stars Lebzelter et al. (2001) find complex and variable profiles indicating strong dynamical effects.

The problem discussed for the second group, namely that the computed gradients close to the short wavelength boundary of the ISO-SWS data are too steep appears also for this class. In general it is even more pronounced, and it could be due to dynamical effects. However, as it was already mentioned, we can not exclude that it is caused by uncertainties of the observations connected to steep energy distributions at the edge of the spectra.

There are two spectra (R Aql, 50358.10 and R Cas, 50458.91) which have a water absorption that is slightly more intense than in the coolest model (2600 K) from our grid. Since they do not look very different and they may be reproduced by a hydrostatic atmosphere with a somewhat lower temperature (2400 to 2500 K), they were included into the third group.

5.4. Type 4

All spectra of Mira stars, where the water absorption is much stronger than in any of our hydrostatic MARCS atmospheres, belong to the last class. The most extreme case in this group with the deepest depression around 2.5 μm is an observation of R Cas (50301.62) which is also presented in Fig. 7. In all spectra of this type the huge opacity of water dominates the whole range below 3.8 μm. The features of CO and OH in this region are not visible or very weak. Large amounts of relatively dense gas with temperatures much cooler than 2000 K are needed in order to explain the enormous intensity of the H_2O bands. It is

clear that such conditions will not appear in any hydrostatic calculation with a realistic choice of the fundamental parameters. On the other hand, in dynamical models for AGB variables (e.g. Höfner & Dorfi 1997; Höfner 1999) the combination of pulsation, dust formation and mass loss produces relatively dense regions in the very extended and cool outer atmospheres around these stars.

In order to explain the behavior of the molecular features in the infrared spectra of cool oxygen-rich giants, Tsuji et al. (1997) introduced one or more dense envelopes situated above a hydrostatic photosphere (warm molecular envelope). Based on this approach Matsuura et al. (2002) produced fits to the ISO-SWS data of several Mira variables covering the range between 2.5 and 4.0 μm. They use two layers of water with different temperatures, column densities and radii described by a disk shape, slab geometry model. For the warmer component they have adopted a value of 2000 K, while the cooler one, which is mainly responsible for the strong depression at 2.5 μm, has between 1000 and 1400 K depending on object and pulsation phase. Although such simple approaches can not replace more detailed studies considering dynamical models for the complex structure of the atmospheres, they still give us a lot of information concerning the basic properties of the gas shells around the stars. This is at least true for the 2.5 μm region, where the water absorption in the layers is optically thick.

As we can see in Table 1 there is one spectrum in this group (R Cas, 50421.06), which shows an emission bump in the region of the SiO bands. However, this feature is weaker than for the data of type 3.

6. Variability of Mira stars

In Table 1 we list the phases of the different ISO-SWS observations of the Mira stars R Aql and R Cas taken from their visual AAVSO light curves. The table also includes the group the corresponding spectrum belongs to as well as information on the appearance of an emission bump in the region of the SiO bands. As it has already been mentioned before, such a feature is visible in all data of type 3. In contrast, the spectra in class 4 have only weak (in one case) or no SiO emission. It is obvious that most of the observations of type 3 were obtained around the time of the visual maximum. All of them have phases above 0.6 or below 0.25. On the other hand the spectra from our sample which belong to group 4 correspond to phases between 0.3 and 0.8. Thus, we see a clear trend that in the two studied Mira variables the most intense water absorption appears around the time of the light minimum, while the weakest 2.5 μm water bands and SiO emission are observed close to the maximum. At a given phase, R Cas always shows the stronger molecular absorption. Due to the limited number and time coverage of our observations it is not possible to determine if the spectral variations exactly follow the visual light curve. Especially for R Cas it is known that the changes of the molecular lines seen in high resolution spectra of the 4 μm range may happen on time scales different from the photometric period (Lebzelter et al. 2001).

Concerning the temporal behavior of the water depression around 2.5 μm our results agree with those of Matsuura et al. (2002) who studied the ISO-SWS data of four Mira stars. They also find that the most intense absorption appears at the time of minimum light corresponding to the largest optical depth of the cool outer H_2O shell in their model of two molecular layers describing the upper atmosphere. Based mainly on the investigation of small scale features, Matsuura et al. conclude that during the phases close to the maximum the water bands in the region between 3.5 and 4 μm may get into emission. In the plots shown in Fig. 7 such a behavior would not be visible, since the fluxes are normalized to the value at 3.8 μm where the total molecular opacity has a minimum. Nevertheless, in cool objects even this point will be affected by the features of water. On the other hand, there is no case among the type 3 spectra in our sample where we need any emission in the 3.5 to 4 μm range to reproduce the overall shape. There are still inversions of some of the small scale structures which do partly also appear in our two Mira stars. However, they could be caused by a major change of the shapes of the bands, which is not necessarily connected to a net emission and may, in contrast to a hydrostatic atmosphere, occur in a dynamical model. Thus, we found no real proof for water emission, but we can not exclude that it influences the small scale features between 3.5 and 4 μm.

7. ISO spectra and linelists for water

The ISO-SWS range between 2.5 and 4 μm is one of the few places where the absorption coefficients calculated from the NASA AMES (Partridge & Schwenke 1997) and our linelist for water disagree. As it was already demonstrated in Paper I, our opacity data reproduce the slopes observed in the corresponding spectra of M-type giants much better. This can also be seen in Fig. 8 where we compare the ISO-SWS measurements of T Sge with theoretical results based on the two lists. At this point it should be noted that the small temperature difference of the models shown in Fig. 8 which is due to the choice of the best fit to the observations will almost not affect the discrepancies. In general it is not possible to remove problems concerning the shape of the H_2O depression by changing the basic stellar parameters of a hydrostatic atmosphere. In Fig. 8 it is also obvious that the observed small scale structure of the water bands in the selected wavelength range can not be reproduced by our list, while the NASA AMES data give significantly better results. This difference was also mentioned in a recent paper on dwarf stars by Jones et al. (2002). It is caused by the fact that for the computation of the line positions Partridge & Schwenke (1997) put much more emphasis on the measurements collected in the HITRAN and HITEMP data base. Unfortunately, the infrared fluxes of the M dwarfs are not sufficient to determine reliable overall slopes from the few existing ISO-SWS spectra. The small scale structure of the water bands predicted by HITEMP and the NASA AMES list is in the investigated frequency range identical. Thus, for the next generation of synthetic spectra we will include more observational material into the determination of the positions of the H_2O lines. However, this will not affect the atmospheric models or the overall shapes of the water features.

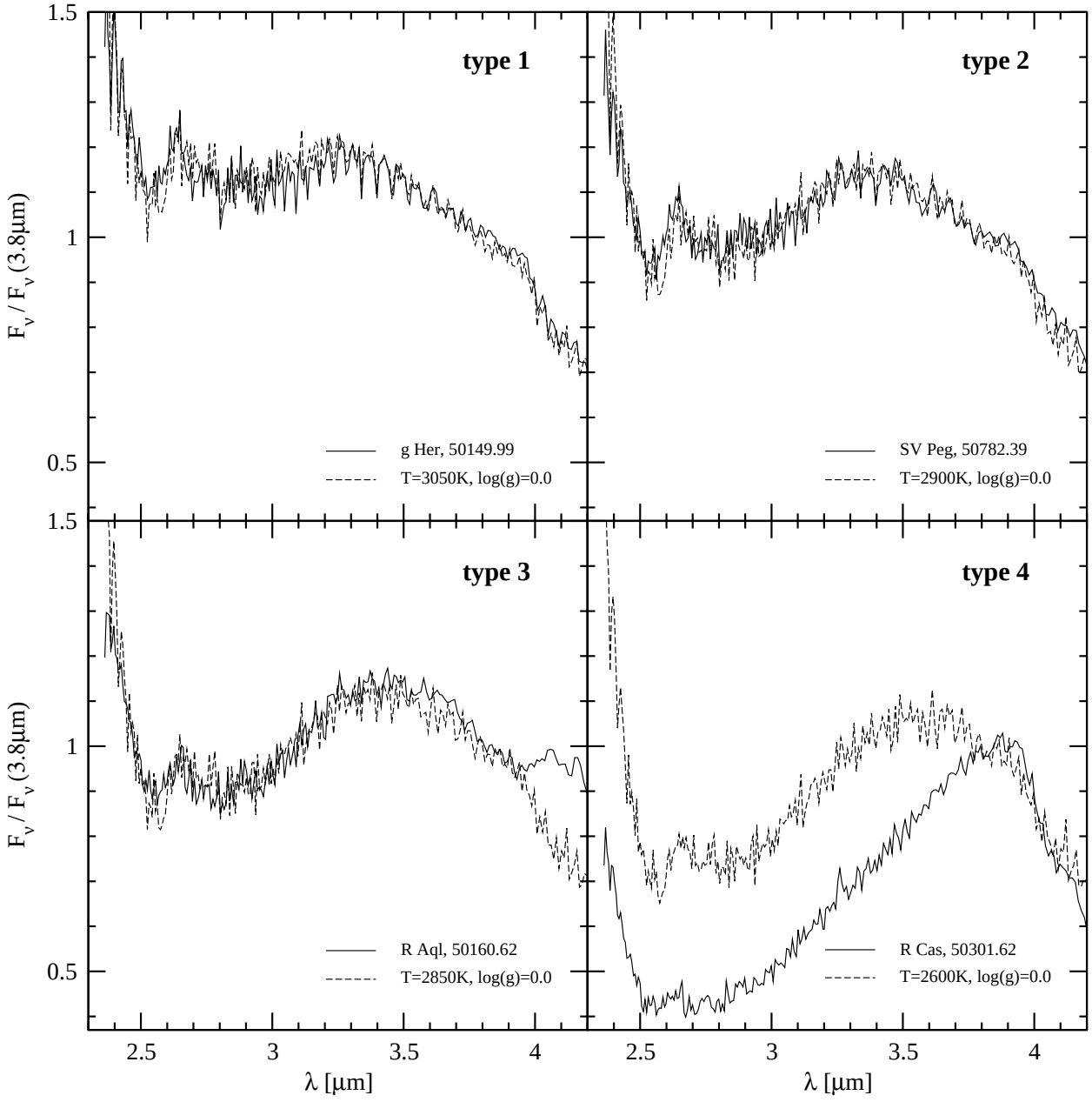

Fig. 7. Comparison of observed and synthetic ISO-SWS spectra for the four groups described in the text. For each class a typical example is shown. The fluxes are normalized to the level at 3.8 μm. The computed spectra are based on MARCS models with one solar mass and solar chemical abundances, which have been selected to give the best fit to the ISO data. They are marked by the corresponding effective temperatures and values of the surface gravity. In addition to the name of the star, the Julian date (JD−2 400 000) is listed for each observation.

8. Conclusions

In this work we present a first systematic comparison between observations and self-consistent model computations of the water bands visible in the 2 to 4 μm spectra of oxygen-rich giants. Such a study has only become possible after an extensive set of good quality data for this type of objects has been obtained by the ISO-SWS instrument. Due to the relatively high infrared fluxes that many of these stars have, the measured slopes in the considered wavelength interval are quite reliable (see Decin et al. 1997 or Loidl 2001) which is an important condition for the investigation of the broad water absorption features. Thus, the agreement between the observed and calculated spectra found for the Semiregular (SRb) and Lb variables in our sample (class 1 and 2) can be regarded as a nice confirmation of the used MARCS atmospheres and opacity data. It should be emphasized again that the model computations are fully self-consistent with no adjustable parameters except for the stellar properties like the surface gravity or the effective temperature which mainly determines the appearance of the H_2O bands in the M-type giants.

In spite of the good agreement between hydrostatic calculations and ISO-SWS observations one should never forget that even for the Semiregular and Lb stars with their relatively weak variations this theoretical approach has some limitations

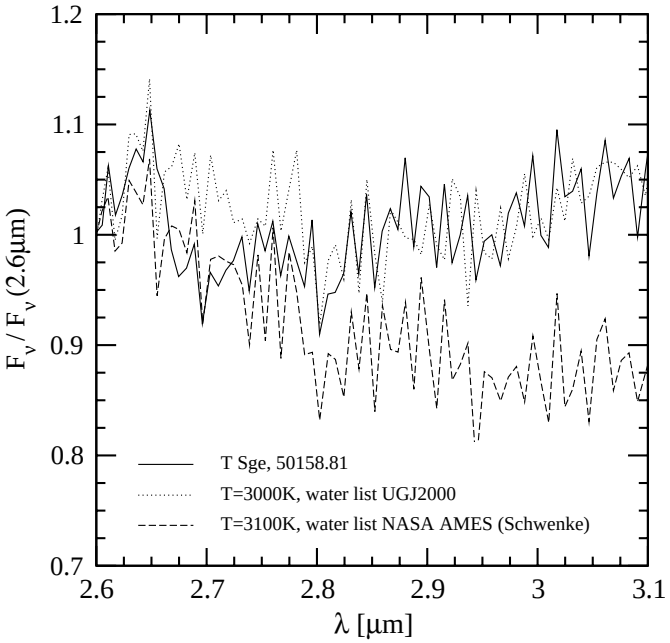

Fig. 8. An observation of T Sge is compared to two synthetic ISO-SWS spectra calculated from MARCS atmospheres using water opacity data taken from the NASA AMES and our linelist. The fluxes are normalized to the value at 2.6 μm. The models have $\log(g[\mathrm{cm/s^2}]) = 0.0$, one solar mass and solar chemical abundances.

regarding the description of the real radial temperature pressure structure, because it neglects important processes like the acceleration of stellar winds or shock waves connected to pulsation. Our results are a quite strong indication that most of the atmospheric regions dominating the molecular absorption in the near and mid infrared (also outside the SWS range) and consequently most of the corresponding band intensities of type 1 and 2 objects can be reproduced by the MARCS models. But we see also prominent exceptions like the features of SiO and perhaps CO which may only be explained by dynamical computations. The strong lines of these species are mainly formed in cool regions far away from the star where the mass loss generates the structure (e.g. Lebzelter et al. 2001; Bessell et al. 1996; Hinkle et al. 1982).

In the case of Mira stars, where the hydrostatic MARCS atmospheres fail to predict the intense water absorption seen around minimum light as well as the SiO emission close to maximum light, it has been shown at several occasions (e.g. Hron et al. 1998; Aringer et al. 1999) that dynamical models may be quite successful in explaining the behavior of different molecular features. However, as it was demonstrated by Höfner (1999) such calculations will only give realistic structures and synthetic spectra, if a non-grey radiative transfer including all relevant opacities is used in a consistent way (the same treatment of opacities for model structure and synthetic spectra). In a subsequent paper of this series we will study the water bands of Mira stars based on dynamical models similar to those published by Höfner (1999), but computed for an oxygen-rich composition.

The fact that the water absorption in the 2.5 μm range observed in Mira stars at phases around maximum light (type 3 spectra) can be reproduced by the MARCS models is not necessarily a coincident. As one would expect, the overall radial dependence of temperature and pressure in a dynamical atmosphere will be very different, which is mainly due to the much larger extension and the appearance of shock waves connected to pulsation (e.g. Höfner et al. 1998). Nevertheless, it is still possible that the conditions in all of the regions dominating the line formation for a certain frequency interval are quite similar in the selected hydrostatic model and the real star. In such cases one will find a good agreement for most of the studied molecular features. Of course, this only proves that a part of the atmosphere looks hydrostatic at a certain time, and it does not tell us anything about the whole structure or other spectral ranges and phases.

Acknowledgements. This work was mainly supported by the Austrian Science Fund Project J 2030 (BA, Schrödinger Fellowship). The work of FK was supported by APART (Austrian Programme for Advanced Research and Technology) from the Austrian Academy of Sciences. UGJ and BA thank the Danish Natural Science Research Council for its support. The ISO Spectral Analysis Package (ISAP) is a joint development by the LWS and SWS Instrument Teams and Data Centers. Contributing institutes are CESR, IAS, IPAC, MPE, RAL and SRON.

References

Anders, E., & Grevesse, N. 1989, Geochim. Cosmochim. Acta, 53, 197
Aringer, B., Jørgensen, U. G., & Langhoff, S. R. 1997, A&A, 323, 202
Aringer, B., Höfner, S., Wiedemann, G., et al. 1999, A&A, 342, 799
Aringer, B. 2000, The SiO Molecule in the Atmospheres and Circumstellar Shells of AGB Stars, Ph.D. Thesis, Univ. Vienna
Bessell, M. S., Scholz, M., & Wood, P. R. 1996, A&A, 307, 481
Cami, J., Yamamura, I., de Jong, T., et al. 2000, A&A, 360, 562
Decin, L., Cohen, M., Eriksson, K., et al. 1997, in Proc. First ISO Workshop on Analytical Spectroscopy, ed. A. M. Heras, K. Leech, N. R. Trams, & M. Perry, ESA-SP 419, 185
de Graauw, T., Haser, L. N., Beintema, D. A., et al. 1996, A&A, 315, L49
Goorvitch, D., & Chackerian, C. Jr. 1994, ApJS, 91, 483
Gustafsson, B., Bell, R. A., Eriksson, K., & Nordlund, Å. 1975, A&A, 42, 407
Hinkle, K. H., Hall, D. N. B., & Ridgway, S. T. 1982, ApJ, 252, 697
Höfner, S., & Dorfi, E. A. 1997, A&A, 319, 648
Höfner, S., Jørgensen, U. G., Loidl, R., & Aringer, B. 1998, A&A, 340, 497
Höfner, S. 1999, A&A, 346, L9
Hron, J., Loidl, R., Höfner, S., et al. 1998, A&A, 335, L69
Jones, H. R. A., Pavlenko, Y., Viti, S., & Tennyson, J. 2002, MNRAS, 330, 675
Jørgensen, U. G. 1992, Rev. Mex. A&A, 23, 195
Jørgensen, U. G., Johnson, H. R., & Nordlund, Å. 1992, A&A, 261, 263
Jørgensen, U. G. 1994, A&A, 284, 179
Jørgensen, U. G. 1997, in Molecules in Astrophysics: Probes and Processes, ed. E. F. van Dishoeck, Proc. IAU Symp., 178, 441 (Kluwer)
Jørgensen, U. G., Jensen, P., Sørensen, G. O., & Aringer, B. 2001, A&A, 372, 249 (Paper I)

Kerschbaum, F., Lebzelter, T., & Lazaro, C. 2001, A&A, 375, 527
Langhoff, S. R. 1997, ApJ, 481, 1007
Lebzelter, T., Hinkle, K. H., & Aringer, B. 2001, A&A, 377, 617
Leech, K. 1998, SWS Instrument and Data Manual, Issue 1.0, ESA Publication SAI/98-095/Dc
Loidl, R. 2001, Spectral Variability of Carbon Stars: A Comparison Between Theory and Observation, Ph.D. Thesis, Univ. Vienna
Matsuura, M., Yamamura, I., Cami, J., Onaka, T., & Murakami, H. 2002, A&A, 383, 972
Nordlund, Å. 1984, in Methods in Radiative Transfer, ed. W. Kalkofen (Cambridge University Press, Cambridge), 211
Partridge, H., & Schwenke, D. W. 1997, J. Chem. Phys., 106, 4618
Plez, B., Brett, J. M., & Nordlund, Å. 1992, A&A, 256, 551
Plez, B. 1998, A&A, 337, 495
Rothman, L. S., Gamache, R. R., Tipping, R. H., et al. 1992, J. Quant. Spectrosc. Rad. Transfer, 48, 469
Ryde, N., Eriksson, K., & Gustafsson, B. 1999, A&A, 341, 579
Schultheis, M., Aringer, B., Jørgensen, U. G., et al. 1999, in Abst. of the 2nd Austrian ISO workshop, Atmospheres of M, S and C Giants, Vienna, Austria, ed. J. Hron, & S. Höfner, 93
Schwenke, D. W. 1997 `http://george.arc.nasa.gov/~dschwenke/oh/oh.html`
Sturm, E., Bauer, O. H., Brauer, J., et al. 1998, Proc. ADASS97, ASP Conf. Ser., 145, 161
Tsuji, T., Ohnaka, K., Hinkle, K. H., & Ridgway, S. T. 1994, A&A, 289, 469
Tsuji, T., Ohnaka, K., Aoki, W., & Yamamura, I. 1997, A&A, 320, L1
Tsuji, T., Aoki, W., & Ohnaka, K. 1999, in Proc. The Universe as seen by ISO, ed. P. Cox, & M. F. Kessler, ESA-SP 427, vol. 1, 229
Valentijn, E. A., Feuchtgruber, H., Kester, D. J. M., et al. 1996, A&A, 315, L60
Windsteig, W., Dorfi, E. A., Höfner, S., Hron, J., & Kerschbaum, F. 1997, A&A, 324, 617
Yamamura, I., de Jong, T., & Cami, J. 1999, A&A, 348, L55